Journal of Environment and Earth Science
ISSN 2224-3216 (Paper) ISSN 2225-0948 (Online)
Vol.6, No.11, 2016

Spatial Distribution of Radionuclides and Major Elements in Soil of Murree and Kotli Sattian Punjab, Pakistan

Khizar Hayat Satti[1] Tania Jabbar[1*] Muhammed Dilband[1] M. Mansha Chaudhry[2] Abdul Jabbar[1] Waheed Arshad[1]
1.Health Physics Division, Pakistan Institute of Nuclear Science &Technology (PINSTECH), Nilore, Islamabad, 45650, Pakistan
2.Department of Nuclear Engineering, Pakistan Institute of Engineering and Applied Sciences, Islamabad, Pakistan

Abstract
The study is aimed to investigate the specific activity of radionuclides and major elements in soils of Subdivisions Murree and Kotli Sattian (Himalayan Mountain range) Pakistan as a part of the ongoing baseline data collection using gamma-ray spectrometer and wavelength dispersive X-ray fluorescence (WDXRF).The natural radionuclides ^{226}Ra, ^{232}Th and ^{40}K showed inhomogenous distribution 20.0 to 29.5, 43.4 to 62.4 and 163.0 to 493.6 Bq kg^{-1} respectively where as ^{137}Cs exhibited extreme variation from 1.3 to 54.1 Bqkg^{-1}. The dominant constitutes of soil were SiO_2, Al_2O_3 and Fe_2O_3. Weak to moderate correlation was observed between elemental composition and activity concentrations of radionuclides. The average annual effective absorbed dose rate measured at 1m above ground due to terrestrial sources was 72.9 ± 1.0 μSvy^{-1}. The high altitude of study area causes the dominant doses to the public .The radium equivalent activity Ra_{eq}, outdoor and indoor hazard indices were lower than the safe limit of Organization for Economic Cooperation and Development report for general public.
Keywords: Gamma emitters, major elements, XRF, soil, Himalayan Mountain range, Gamma Spectrometry

1 Introduction

The assessment of natural (accounted for 50-80% of the gamma radiation flux at the soil surface) and anthropogenic radionuclides is necessary to evaluate the risks arising from radiations (Izquierdo et al., 2011). Naturally occurring radionuclides of terrestrial origin like members of the ^{238}U and ^{232}Th series, together with ^{40}K, and their concentrations in soil are related to the nature of the parent rock during soil genesis. Their natural radioactivity levels vary depending on the geological and geographical structure (Vukasinovic, DJORDJEVIC et al. 2010). It has been observed that granitic rocks contain higher amounts of thorium, uranium and light rare earth elements (REEs) compared to other igneous rocks such as basalt and andesites (SAHOO, HOSODA et al. 2011). Anthropogenic radionuclides are introduced into environment mainly from nuclear releases and nuclear weapon tests performed in early 1960's and dispersed through atmosphere.^{137}Cs a fission product with high fission yield and half-life of 30 years, is a prominent indicator of nuclear releases (Izquierdo et al., 2011).

Soil play a major role in the cycling of radionuclides and their physicochemical properties influence the mobility and bioavailability of these radionuclides in terrestrial ecosystems (Izquierdo et al., 2011). The concentration and composition of elements in the soil are also of primary importance in determining distribution of any radionuclide between soil particle and soil solution. Radionuclides are adsorbed onto soil components (organic matter, clays, carbonates, Fe/Mn oxides) and take part in biogeochemical processes.

The objective of this study was to determine spatial distribution of primordial (^{226}Ra, ^{232}Th and ^{40}K) and anthropogenic ^{137}Cs in the study area of Murree and Kotli sattian to provide a baseline data for future reference. In addition, the composition of parent materials in the study area, might explain the distribution of radionuclides in the landscape.

2 Materials and Methods

2.1 Geology of study area

The sampling was carried out in subdivisions Murree and Kotli sattian, hilly areas of District Rawalpindi of Punjab province. The study area is situated at 33^{0}35$^/$-33^{0}54$^/$ latitude and 73^{0}26$^/$-73 ^{0} 27$^/$ longitude and is the one of the most popular tourists destination in Pakistan. The total area is approximately 762 km^2. The Murree is known as "Queen of Hills''. The hills of Kotli sattian are at the edge of the Himalayan Mountain range of Miocene sand stone and Eocene MUMMULTIC lime stone (Satti 2000).The Murree formation at some places is purple to reddish brown, medium grained thin bedded hard sand stone contains of chert. The important rocks of this area include limestone, shale, sandstone, brick-red clay, silty clay stone and purple to dark brown sand stone (Kazmi and Jan, 1997). The average rainfall per annum is 1789 mm. The elevation of study area ranges from 2000 to 7200 feet above sea level.

2.2 Sample collection and Analysis

The sampling area was divided into grids (5 × 5 km^2) on equidistant basis as shown in fig1. At each sampling site an area of dimensions 2m × 2m was selected, after removing top vegetation cover, four subsamples were taken from corners of square and one from center. These samples were taken with the help of coring tool (2 cm diameter and 5cm coring length) at depth of (0-5) cm. These subsamples were pulverised manually to get a homogenized sample. Site locations were identified using a portable global positioning system (GPS) as presented in Table 1.

The soil samples were dried, powdered, mixed and passed through 2 mm mesh sieve (IAEA, 1989). The samples were stored for more than 22 days to establish secular equilibrium of ^{238}U with its progeny. The radiometric analysis of samples was carried out using a high-resolution coaxial high purity germanium detector (HPGe) Model GC2519 for 65000 seconds. The detector had graded shielding (15 cm thick lead having inner lining of 3 mm thick copper and 4 mm thick tin) to reduce the background by increasing backscattering (Knoll, 2010) . GENIE-2000 software was used for spectral analysis. The activity concentration of the ^{226}Ra and ^{232}Th were estimated using the photo-peaks of their daughters (^{214}Pb 351 keV and ^{214}Bi 609,1120 keV) and (^{228}Ac, 911keV). Photo-peaks at 662 and 1460.8 keV were used for ^{137} Cs and ^{40}K activities respectively. The minimum detectable activity values for ^{226}Ra, ^{232}Th, ^{40}K and ^{137}Cs were 3.60, 2.25, 6.70 and 1.10 $Bqkg^{-1}$ respectively. The quality control was assured using reference soils IAEA 375, IAEA 327 and soil 6.

For chemical composition, sieved samples were mixed with binder (4:1) and palletized in aluminum cap (diameter 37 mm) with help of 150 kN hydraulic press. Each sample was irradiated for 300 sec. The concentrations were measured against rock standard RG-1, RGN-1. The chemical analysis was performed using Axios Sequential XRF spectrometer. The instrument was operated at 4 kW power and equipped with a SST X-ray tube technology, Rh anode and LiF-200 crystal (for dispersion of wavelengths).

3 Results and discussion

3.1 Activity Concentrations

The measured concentrations of ^{226}Ra, ^{232}Th, ^{137}Cs and ^{40}K on dry weight basis with uncertainties at 1 sigma level are shown in Table 2. The mean specific activities of terrestrial radionuclides ^{226}Ra, ^{232}Th, and ^{40}K were 24.7 ± 2.9, 52.5 ± 4.9 and 368 ± 75.0 Bq kg^{-1} respectively with ranges (20-30), (43-63) and (163-493) Bq kg^{-1} respectively. However, ^{137}Cs concentration showed large variation from 54.1± 0.8 $Bqkg^{-1}$ in KotliRF to 1.3 ± 0.1 Bq kg^{-1} in Samli colony respectively.The quantitative analysis of data by Anderson Darling test showed that all the radionuclides ^{226}Ra (p-value=0.4), ^{232}Th (p-value=0.8), and ^{40}K (p=0.1) except Cs-137 (p- value < 0.05) were normally distributed about their mean with 95% confidence level.

The activity concentrations of primordial radionuclides were observed to follow order as: $^{226}Ra < ^{232}Th < ^{40}K$. The average values of activity concentration in Bq kg^{-1} were converted in units of part per million (ppm) for U and Th and % for ^{40}K using conversion factors reported in literature. The average values obtained were 2.0 ± 0.01 ppm of uranium, 12.7 ± 0.14 ppm of thorium and 1.2 ± 0.01% of ^{40}K. These values are comparable to those for shales of sedimentary origin (Tyler, 1994).

The $^{232}Th/^{226}Ra$ activity ratio (i.e., progeny pair $^{228}Ac/^{214}Pb$) can be used to assess the maintenance of the proportionality within the ^{232}Th and ^{226}Ra decay series, which in most environmental samples is about 1.1. In our study, $^{232}Th/^{226}Ra$ was found to vary from 1.6 to 2.6 with mean value 2.1. ^{232}Th can be easily mobilized in forms of various complex inorganic cations and organic compounds, it is expected that leaching and sorption might be attributed to different mobility of ^{232}Th and ^{226}Ra (Izquierdo et al., 2011) as reported for ^{238}U.

A comparison of present data with other hilly areas of Pakistan i.e. Hunza (Ali et al., 2013), Mirpur (AJK) (Rafique et al., 2011) and Swat (Jabbar et al., 2008) was also made through Box-Whisker plots as shown in Fig. 2 a-d. Hunza is located in the sedimentary belt of Karakorum mountains range. The rocks of Hunza are composed of limestone, conglomerates, quartzite, marble, schist, gneiss. The Mirpur formation consists of a conglomerate as a major unit with some mudstones or sand stones and lies on Himalayan mountain range as study area. Swat is located in Kohistan mountain range. The granite gneiss of swat consists of feldspar, biotite, garnet and chlorite (Kazmi and Jan, 1997).

From Fig. 2-a it can be seen that the average activity concentration of ^{226}Ra was comparable to Mirpur but lower than values reported for Hunza and Swat. However, activity concentration in the study area covers a narrow range than all the other hilly stations compared. Quite similar to ^{226}Ra, ^{232}Th concentrations were also comparable to Mirpur and may be attributed to same geology. The average activity concentration of ^{40}K was lowest in the study area. Although concentration was comparable to Swat but data had still overlapping with Mirpur. Of the radionuclides detected, ^{137}Cs had the most heterogeneous distribution in study area contrary to other compared areas where it was below MDA for most of sampling sites.

3.2 Comparison with World's Data

A comparison of baseline data obtained in the present study with some countries in East Asia is shown in Table

3. It can be seen that average activity of terrestrial radionuclides are comparable to China, Thailand and Kazakhstan, lower those measured in Kauman Himalaya and Malaysia.^{137}Cs data was not available for most of countries compared except Kauman Himalaya. The average ^{137}Cs activity levels in present study area were higher than those found at Kauman Himalaya.

3.3 Chemical Composition

There are many physical and chemical factors that are not only responsible for the distribution of radionuclides in soil but also responsible for surface and sub-surface alterations. Therefore, few samples (grids size 10 × 10 km^2) were analyzed by XRF for soil chemistry.

The chemical composition of soil samples was expressed as the function of eight major elements. Their concentration in terms of their respective oxides is represented by their weight percentage as shown in Table 4.The average values of major elements are given in terms of one standard deviation.

It s evident that the concentration of SiO_2 in the study area vary from 58.7 to 71.3 % with an average value of 66.2 ± 3.9 %. TiO_2 concentration had homogenous distribution in soil of study area and was found in range (0.8% -1.4%), consistent with the range value (0.5-1.5) reported by (Omoniyi et al., 2013). The average value of Al_2O_3 was estimated to be 16.2 ± 1.6 with the values ranging from 13.1-17.9%. Fe_2O_3 was found to be varying from 3.4 to 7.9%. Similarly, the mean concentrations of MnO, MgO, CaO and P_2O_5 were estimated to be 0.1, 2.93, 4.4, 0.2% respectively.

3.4 Correlation Study

Correlation study using linear regression model was carried out between radionuclide concentration and major stable elements as variables. Microsoft Excel 2007 was used to perform the correlation study. Weak to moderate correlations were observed. These moderate correlations include ^{137}Cs-Fe_2O_3 (r = 0.7), ^{40}K-Fe_2O_3 (r = 0.8), ^{40}K-Al_2O_3 (r=0.8) see Fig. 3 a, b & c.

The data did not represent any significant correlation between silicates and terrestrial radionuclides in the study area. A Moderate correlation between ^{137}Cs and Fe_2O_3 revealed that major soil constituents responsible for the retention of cesium are clay, silt and Fe oxides. McKay and Baxter (1985) showed that the presence of oxides and organics was important in the soil thus preventing the release of ^{137}Cs from the clay mineral fractions. Therefore, clay soil acts as a sink for ^{137}Cs (Tyler, 1994).

3.5 Radiological parameters

Radium Equivalent activity and hazard indices

Most of the houses in the present study area are being constructed by using local rocks, walls and floors are labeled with mud and roofs are also covered by soil. So, people are exposed to radiation indoor as well as outdoors. The weighted sum of ^{226}Ra, ^{232}Th and ^{40}K activities, frequently used for the estimation of radiation hazards in building materials, is quantified by radium equivalent activity (Ra_{eq}) (Beretka and Mathew 1985). It is defined by following relation

$$Ra_{eq}(Bq\ kg^{-1}) = A_{226Ra} + 1.429\ A_{232Th} + 0.077\ A_{40K} \quad (1)$$

Where, A_{226Ra}, A_{232Th} and A_{40K} are activity concentrations of ^{226}Ra, ^{232}Th and ^{40}K in Bq kg^{-1} respectively. Any material is potentially radiotoxic if the value of Ra_{eq} exceeds 370 Bq kg^{-1} corresponds to annual effective dose of 1.05 mSv. The brief statistics of radium equivalent activity values are shown in Table 5. The values vary from (107.3-147.8) with average value of 126.6 ± 9.5 Bqkg^{-1} which is 66% lower than safe limit of 370 Bq kg^{-1}.The main contributor to Ra_{eq} in study area was ^{232}Th with average 58% contribution.

The hazards associated with outdoor or indoor occupancy are represented by outdoor radiation hazard index H_{out} and H_{in} respectively(Beretka and Mathew, 1985). These indices are calculated by using following formulae

$$H_{out} = (A_{226Ra} / 370) + (A_{232Th} / 259) + (A_{40K} / 4810) \quad (2)$$

$$H_{in} = (A_{226Ra} / 185) + (A_{232Th} / 259) + (A_{40K} / 4810) \quad (3)$$

Its value also should be less than one. It can be seen from Table 5 that maximum values of H_{in} and H_{out} were found at DewalRF but still these values are less than unity.

Annual effective dose

The annual effective dose due to background radiations may be regarded as the sum of doses from terrestrial radionuclides (^{226}Ra, ^{232}Th and ^{40}K), anthropogenic radionuclides (^{137}Cs) and cosmic radiations. The air absorbed dose rate at one meter above ground due to terrestrial radiations is given by (Singh et al., 2009)

$$D\ (nGyh^{-1}) = 0.461A_{226Ra} + 0.623\ A_{232Th} + 0.0414\ A_{40K} \quad (4)$$

The outdoor annual effective dose equivalent can be calculated by using following relation (Khan et al., 2012)

$$E_{out}\ (\mu Svy\text{-}^{1}) = 0.7 \times D\ (nGyhr^{-1}) \times 0.2 \times 8760 \times 10^{-3} \quad (5)$$

Where, E_{out} is outdoor effective dose equivalent, 0.7 (SvGy^{-1}) is Sievert to Grey conversion factor, 0.2

is outdoor occupancy factor. Since atomic weapon testing in early sixties and the accident of Chernobyl and Fukushima, ^{137}Cs is unevenly distributed throughout the world and its higher levels may produce significant exposures to mankind. The effective dose rate at one meter above ground contributed by ^{137}Cs, neglecting air attenuation, can be calculated by using equation 6 as given in (Cember and Johnson, 2000)

$$D_{137Cs}\ (\mu Svh^{-1}) = 0.576\ E^{*}\ \Phi\ ^{*}(\mu_a/\rho)^{tissue} \times 10^{-3} \quad (6)$$

Where, E is gamma ray energy of ^{137}Cs photon, $(\mu_a/\rho)^{tissue}$ is energy dependent mass attenuation coefficient of soft tissue and has value 0.0316(cm^2/gm). Φ is gamma ray flux at one meter above ground and is given by

$$\Phi = \frac{A*Y}{2*(\mu a/\rho)^{soil}} \quad (7)$$

Where, A is activity of ^{137}Cs in $Bqkg^{-1}$, Y is gamma ray emission probability per disintegration of ^{137}Cs, 2 in the denominator is due to fact that one half of the total emitted photons form soil probably move upward and $(\mu_a/\rho)^{soil}$ is mass attenuation of soil. The value of mass attenuation coefficient of at 661 keV of ^{137}Cs was measured using gamma ray transmission method (Cutshall et al., 1983). The average value of mass attenuation coefficient was found to be 0.0780 cm^2/ g. The outdoor annual effective dose rate was calculated by equation 8 as,

$$E_{137Cs} = D_{137Cs}\ (\mu Svhr^{-1}) \times 8760 \times 0.2 \quad (8)$$

The average value of the outdoor annual effective dose rate due to ^{137}Cs in soil came out to be 1.9±0.02 which is 63% of world's average reported value of $3\mu Svy^{-1}$. Table 6 represents the brief statistics. The dose contribution from ground deposition of ^{137}Cs was insignificant. The component of annual effective dose from directly ionizing cosmic radiation and that from neutron part as the function of altitude above sea level can be expressed by equations 9 and 10 respectively (UNSCEAR, 2000).

$$\dot{E}_{DI} = \dot{E}(0)\ [\ 0.79\ \exp(0.4528z) + 0.21\ \exp(-1.649z)] \quad (9)$$

$$\dot{E}_N = 1.98\ \dot{E}_N(0)\ \exp(0.698z) \quad (10)$$

Where, $\dot{E}(0)$ is annual effective dose from comic radiations at sea level, $\dot{E}_N(0)$ is annual effective dose from neutron part at sea level and z is altitude above sea level in kilometers. The cumulative dose that a person may receive during a year is the sum of all these contributions

$$E_{net} = E_{terr} + E_{cos} + E_{Cs\text{-}137} \quad (11)$$

It can be seen from Table 6 that average annual effective dose 72.0 ± 1.0 μSvy^{-1} is comparable to world's average. However, outdoor dose contribution from cesium part came out to be 46% lower than world's average value. The most dominate term to annual effective dose rate came from cosmic radiations which was 87% of total annual effective dose thus 32% higher than world's average value. Clearly, this is attributed to higher altitudes of the study area.

4 Conclusions

The data obtained revealed that the concentration of radionuclides and major stable elements vary considerably from one site to the other . The activity concentrations of primordial radionuclides showed that soil of study area might have originated from sedimentary shale. The $^{232}Th/^{226}Ra$ activity ratios as a measure of disequilibrium caused by the different mobility of the radioisotopes provided insights into the intensity of soil processes. The chemical analysis confirmed that the study area was rich in silicates and alumina. Weak to moderate correlation was found between major elements and radionuclide concentrations. The outdoor and indoor radiation hazard indices exhibited that the soil of study area was hazard free. The annual effective dose rate due to terrestrial radionuclides was comparable to world's average value. The major dose contribution to total annual effective dose came from cosmic radiations due to high altitudes of study area and was 32% higher than World's average value. The dose contribution from ^{137}Cs part may be neglected. Nevertheless, two sampling locations KotliRF and Bariyan were identified to have relatively higher values of ^{137}Cs concentration.

5 References

Ali, M., Iqbal, S., Wasim, M., Arif, M., Saif, F., 2013. Soil radioactivity levels and radiological risk assessment in the highlands of Hunza, Pakistan. Rad. Prot. Dosim. 153 (3), 390-399.

Beretka, J., Mathew, P., 1985. Natural radioactivity of Australian building materials, industrial wastes and by-products. Health Phys. 48 (1), 87-95

Cember, H., Johnson, T., 2000. Introduction to Health Physics. 4th Edition, McGraw-Hill New York.

Cutshall, N., Larsen, , I.L., Olsen, C.R., 1983. Direct analysis of Pb-210 in sediment samples: a self-absorption corrections. Nucl. Instr. and Meth. A 206, 309-312.

International Atomic Energy Agency IAEA, 1989. Measurement of radionuclides in food and environment. Technical Report Series No. 295, Vienna.

Izquierdo, N.A., Gaspar, L., López-Vicente, M., Machín, J., 2011. Spatial distribution of natural and artificial radionuclides at the catchment scale (South Central Pyrenees). Rad. Meas. 46 (2), 261-269.

Jabbar, T., Khan, K., Subhani, M., Akhter, P., Jabbar, A., 2008. Environmental gamma radiation measurement in District Swat, Pakistan. Rad. Prot. Dosim. 132 (1), 88-93

Kazmi, A.H., Jan, M.Q., 1997. Geology and tectonics of Pakistan, Graphic publishers Karachi

Khan, K., Khalid, M.R., Jabbar, A., Akhter, P., 2012. Appraisal of radioactivity and associated radiation hazards in sand samples of four rivers of Punjab province, Pakistan. Isot.Environ. Healt. S. 48 (2), 286-294

Knoll, G.F., 2010. Radiation detection and measurement, John Wiley & Sons

Omoniyi, I.M., Oludare, S.M., Oluwaseyi, M., 2013. Determination of radionuclides and elemental composition of clay soils by gamma-and X-ray spectrometry. SpringerPlus 2 (1), 1-11

Rafique, M., Rehman, H., Malik, F., Rajput, M., Rahman, S., Rathore, M., 2011. Assessment of radiological hazards due to soil and building materials used in Mirpur Azad Kashmir; Pakistan Iran. J. Radiat. Res.9 (2), 77-87

Sahoo, S.K., Hosoda, M., Kamagata, S., Sorimachi, A., Ishikawa, T., Tokonami, S., Uchida, S., 2011. Thorium, uranium and rare earth elements concentration in weathered Japanese soil samples. Nucl. Sci.Technol. 1, 416-419.

Satti, S. 2000. A Hand Book of Kotli Sattian. Nanopathy

Singh, J., Singh, H., Singh, S., Bajwa, B., Sonkawade, R., 2009. Comparative study of natural radioactivity levels in soil samples from the Upper Siwaliks and Punjab, India using gamma-ray spectrometry. J. Environ. Radioac. 100 (1), 94-98

Tyler, A N., 1994. Environmental influences on gamma ray spectrometry, Ph. D. Thesis, The Science Faculty, University of Glasgow

UNSCEAR 2000. Sources and effects of ionizing radiation, United Nations Scientific Committee on the Effects of Atomic Radiation, United Nations, New York.

Vukasinovi, I., Dordevic, A., Rajkovic, M.B., Todorovic, D., Pavlovic, V.B., 2010. Distribution of natural radionuclides in anthrosol-type soil. Turk. J. Agric. For. 34, 539-54

Table 1 Geographical data of sampling points

Sr.No.	Sample ID.	Sample Location	Coordinates	Altitude (ft)
1.	I.	Newala	33.88 N ,73.58 E	2287
2.	II.	Bahndi	33.88 N ,73.54 E	3438
3.	III.	Kamra	33.73 N, 73.50 E	4089
4.	IV.	Bhattian	33.75 N, 73.49 E	3782
5.	V.	Bariyan	33.96 N, 73.39 E	6980
6.	VI.	Dhar RF	33.93 N, 73.39 E	5890
7.	VII.	Sambli colony	33.72 N, 73.35 E	2431
8.	VIII.	Nanjan	33.74 N,73.39 E	3755
9.	IX.	Patriata	33.85 N, 73.48 E	7280
10.	X.	Messyari	33.87 N,73.44 E	5843
11.	XI.	Tarmina	33·80 N ,73.23E	2282
12.	XII.	Arokas	33.84 N,73.29 E	2926
13.	XIII.	Kotli RF	33.82 N ,73.52 E	3960
14.	XIV.	Barhad	33.80 N,73.55 E	2574
15.	XV.	DewalRF	33.98 N, 73.46E	5940
16.	XVI.	Talut	34.03 N,73.85 E	3630
17.	XVII.	Suleha	33.78 N ,73.40E	2546
18.	XVIII.	Balkh	33.80 N,73.33 E	3585
19.	XIX.	Lawrence college	33.88 N, 73.36E	5730
20.	XX.	Ghora Gali	33.81 N,73.33 E	4505
21.	XXI.	Charra pani	33.85 N,73.32E	3610
22.	XXII.	Sambli Behra mal	33.83 N,73.37 E	3774
23.	XXIII.	Sanj	33.84 N,73.45 E	4889
24.	XXIV.	Durbhandi	33.79 N,73.45 E	4935
25.	XXV.	Chapprian	33.93 N,73.55 E	2206
26.	XXVI.	Gohi Rf	33.93 N,73.50 E	2896
27.	XXVII.	Kashmiri Bazar	33.94 N,73.45 E	6386
28.	XXVIII.	Kuthian	33.84 N,73.54 E	3979
29.	XXIX.	Sarmandal	33.84 N,73.49 E	6596
30.	XXX.	Behl	33.75 N,73.43 E	3436
31.	XXXI.	Channeri	33.74 N,73.33E	2934

Table2: Activity concentration of Radionuclides in soil samples

Sr .No.	*Sample ID*	*Activity Concentration (Bqkg^{-1})*			
		^{226}Ra	^{232}Th	^{137}Cs	^{40}K
1.	I	24.3 ± 1.5	53.7 ± 5.8	6.3 ± 0.4	377.4 ± 23.3
2.	II	26.2 ± 1.3	52.3 ± 4.6	9.7 ± 0.4	421.1 ± 20.5
3.	III	27.7 ± 1.0	57.9 ± 2.6	10.3 ± 0.3	472.4±22.8
4.	IV	25.9 ± 1.4	54.7 ± 3.2	13.6 ± 0.4	435 ± 23.1
5.	V	28.9 ± 1.1	49.3 ± 2.0	38.3 ± 0.7	424.8±23.2
6.	VI	27.8 ±1.0	48.6 ± 2.1	23.6 ± 0.3	349 ± 18.6
7.	VII	29.5±0.9	51.9 ± 3.1	1.3±0.1	163.1±16.2
8.	VIII	25.4 ± 1.1	55.3 ± 4.1	4.7 ± 0.1	456 ± 25.7
9.	IX	20.0±0.8	43.4 ± 3.1	3.6±0.2	374.4±17.5
10.	X	22.7 ± 0.9	48.4 ± 3.7	2.7 ± 0.1	409 ± 20.8
11.	XI	21.5± 0.9	45.1 ± 3.4	2.3±0.1	276.8±19.9
12.	XII	23.4 ± 1.3	60.4 ± 4.8	16.6 ± 0.3	344 ± 19.1
13.	XIII	20.6±0.9	45.5 ± 3.7	54.1±0.8	493.6±21.1
14.	XIV	28.5 ± 1.5	49.9 ± 3.1	30.6 ± 0.7	417 ± 22.3
15.	XV	27.0±1.0	62.4 ± 4.1	26.4±0.5	410.8±22.9
16.	XVI	29.4 ± 1.3	47.7 ± 2.8	10.6 ± 0.4	234 ± 17.6
17.	XVII	25.4±1.0	54.6 ± 4.0	3.8±0.2	288.1±19.0
18.	XVIII	22.2 ± 0.8	55.8 ± 4.2	24.34 ± 0.5	376 ± 20.3
19.	XIX	23.8±0.9	50.6 ± 3.9	20.8±0.5	397.9±21.4
20.	XX	24.1 ± 0.9	48.9 ± 3.2	11.7 ± 0.3	387 ± 21.2
21.	XXI	27.6 ± 1.2	44.3 ± 2.9	14.4 ± 0.3	287 ± 18.7
22.	XXII	26.5 ± 1.3	57.2 ± 4.1	8.3 ± 0.2	295 ± 19.3
23.	XXIII	21.3 ± 0.9	48.5 ± 3.1	15.9 ± 0.4	411 ± 22.1
24.	XXIV	23.9 ± 1.2	44.6 ± 2.7	3.9 ± 0.2	348 ± 19.7
25.	XXV	29.1 ± 1.2	50.7 ± 3.3	12.8 ± 0.2	435 ± 23.7
26.	XXVI	20.5 ± 0.8	47.8 ± 2.8	17.6 ± 0.3	408 ± 22.6
27.	XXVII	23.2 ± 0.9	60.5 ± 4.0	4.8 ± 0.2	312 ± 16.6
28.	XXVIII	25.1 ± 1.3	56.4 ± 3.7	4.2 ± 0.3	457 ± 25.3
29.	XXIX	20.5 ± 1.1	43.9 ± 2.7	9.3 ± 0.4	421 ± 23.4
30.	XXX	23.6 ± 1.4	45.7 ± 3.4	2.8 ± 0.1	342 ± 22.3
31.	XXXI	21.5 ± 0.9	53.8 ± 3.6	13.7 ± 0.5	287 ± 18.3

Table 3 Comparison with World's Data

Country	^{226}Ra	^{232}Th	^{40}K	^{137}Cs
China	32	41	440	--
India	29	64	400	--
Bangladesh	34	--	350	--
Malaysia	67	82	310	--
Kazakstan	35	60	300	--
Thailand	48	51	230	--
Japan	33	28	310	--
Kauman Himalaya, India	67	79	887	2.8
Punjab, Pakistan	35	41	615	2.8
Gilgit	25	29	115	3.6
Hunza	60	59	766	2.2
Ghanger Valley	56	58	852	13.4
Sawat				
World's Median	400	35	30	--
Present study	25	53	368	13.6

Table 4 Concentration of major elements in soil samples

Sample ID	*SiO2*	*TiO2*	*Al2O3*	*Fe2O3*	*MnO*	*MgO*	*CaO*	*P2O5*
I	69.1	1.2	16.9	6.5	0.1	2.4	2.6	0.1
III	67.0	1.2	17.6	6.2	0.1	2.7	2.9	0.1
V	64.0	1.3	16.0	7.4	0.2	8.5	2.3	0.1
VII	71.3	1.4	14.4	4.3	0.1	1.1	3.5	0.8
IX	70.0	1.2	17.4	7.0	0.1	1.7	1.4	0.6
XI	58.7	0.8	13.1	3.4	0.1	2.0	18.5	0.1
XIII	62.0	1.3	17.7	7.9	0.2	3.9	3.0	0.1
XV	69.5	1.3	16.5	6.3	0.1	2.4	1.0	0.2
XVII	66.2	1.0	14.7	3.9	0.1	2.3	7.1	0.1
XIX	64.0	1.4	17.9	7.2	0.2	2.2	2.0	0.1

Table 5 Radiological parameters estimated from soil of study area

Statistics	Ra_{eq} ($Bqkg^{-1}$)	H_{in}	H_{out}
Minimum	107.3	0.3	0.3
Maximum	147.8	0.5	0.4
Mean	126.6	0.4	0.3
Geometric Mean	127.9	0.4	0.3
Median	128.5	0.4	0.3
Permissible value	370	1	1

Table 6 Annual effective dose rate components

Statistics	E_{terr}(μSvy^{-1})	E_{cos}(μSvy^{-1})	E_{Cs-137} (μSvy^{-1})
Minimum	60.7	368.7	0.1
Maximum	83.9	798.9	6.2
Mean	72.0	503.8	1.6
Geometric Mean	71.8	490.7	1.2
Median	71.5	459.4	1.1
World's average	70.0	380	3.0

List of Figures

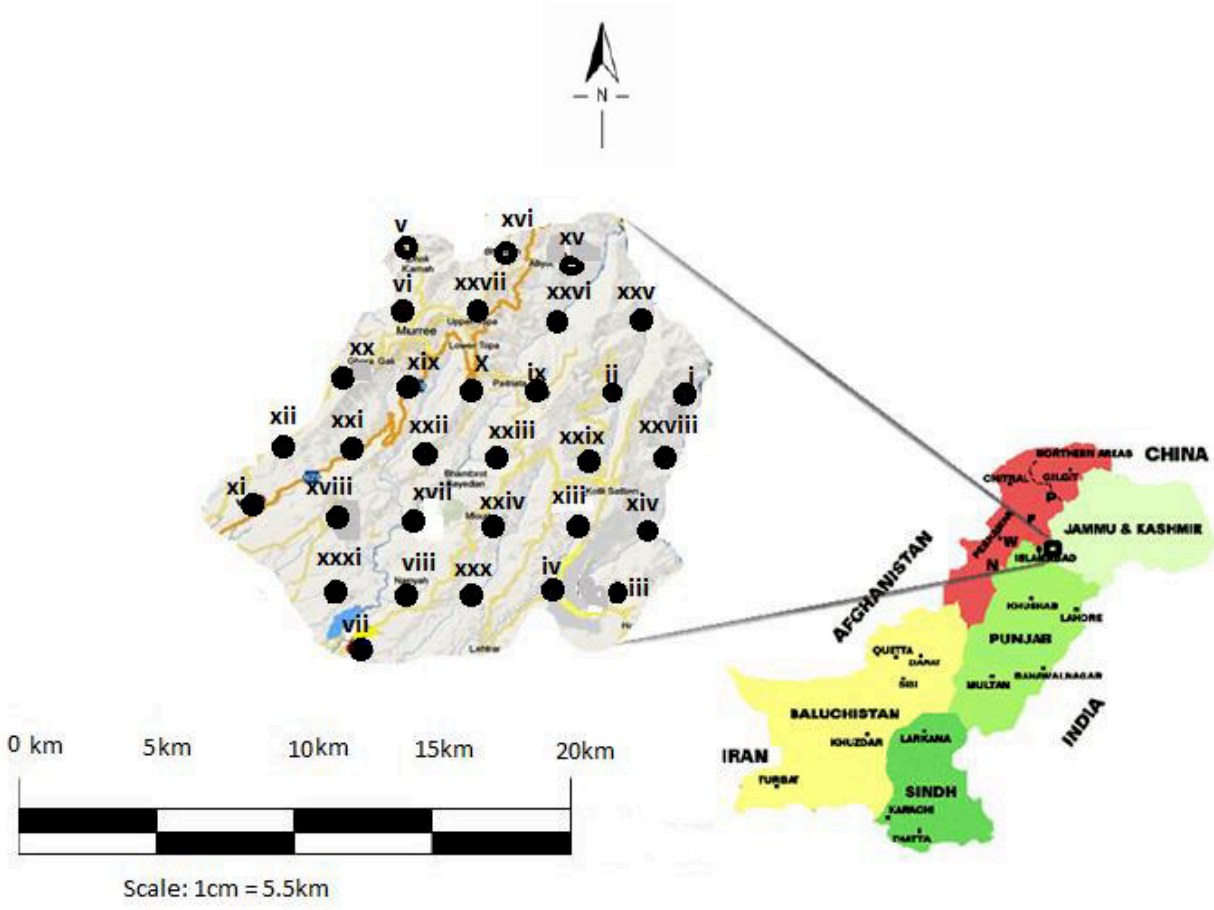

Fig.1 Study area

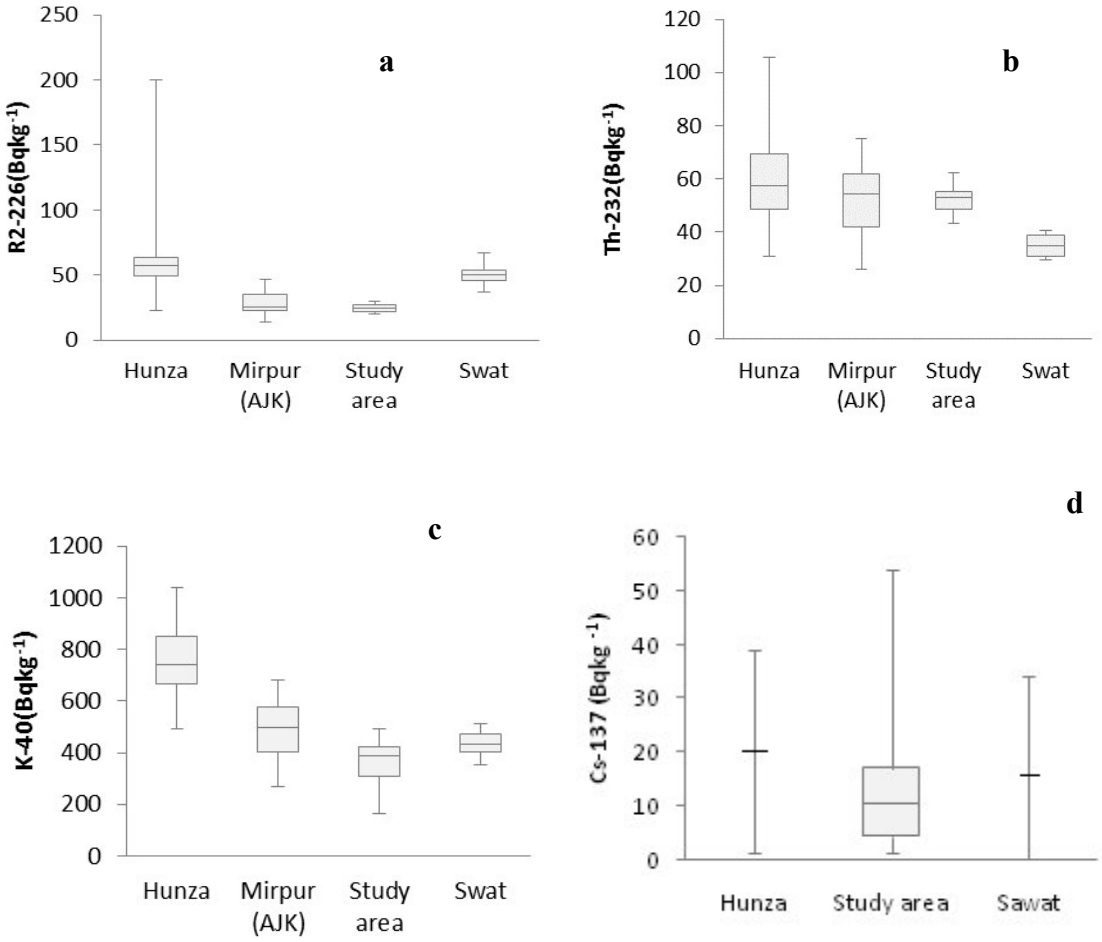
a
R2-226(Bqkg-1)
250
200
150
100
50
0
Hunza
Mirpur (AJK)
Study area
Swat
b
Th-232(Bqkg-1)
120
100
80
60
40
20
0
Hunza
Mirpur (AJK)
Study area
Swat
c
K-40(Bqkg-1)
1200
1000
800
600
400
200
0
Hunza
Mirpur (AJK)
Study area
Swat
d
Cs-137 (Bqkg-1)
60
50
40
30
20
10
0
Hunza
Study area
Sawat

Fig. 2

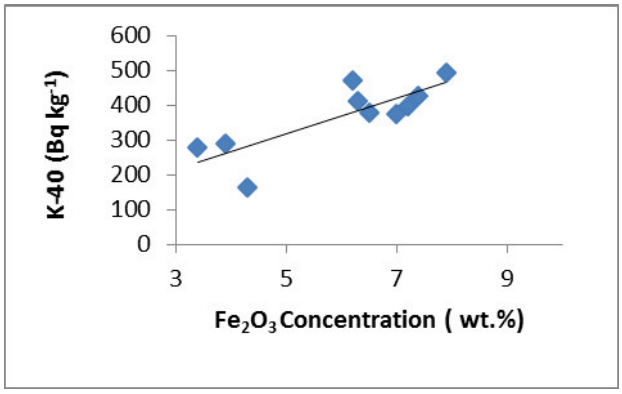
600
500
400
300
200
100
0
K-40 (Bq kg-1)
3
5
7
9
Fe2O3 Concentration (wt.%)

a

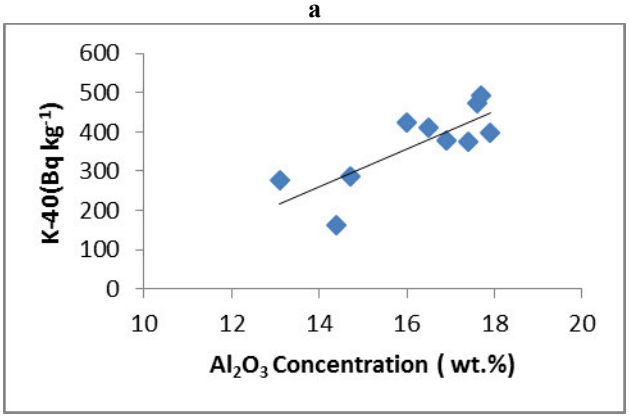
600
500
400
300
200
100
0
K-40(Bq kg-1)
10
12
14
16
18
20
Al2O3 Concentration (wt.%)

b

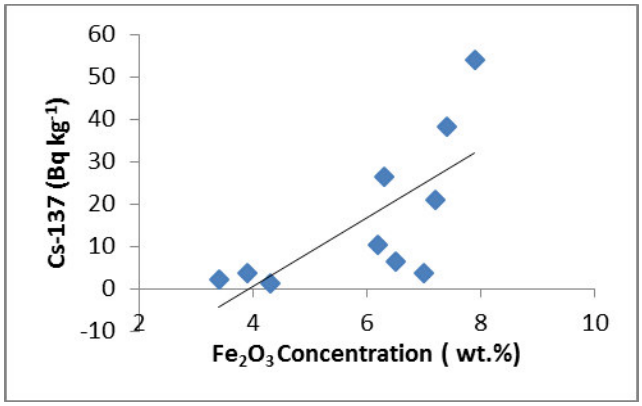
60
50
40
30
20
10
0
-10
Cs-137 (Bq kg-1)
2
4
6
8
10
Fe2O3 Concentration (wt.%)

c

Fig. 3